

# Numerical prediction of methane- and biogas-fuelled power generation

Mohamed Hamdi <sup>#1</sup>, Ahmed Taieb <sup>\*2</sup>

<sup>#</sup> *Laboratory of Wind Power Control and Energy Valorization of Waste, Research and Technology Center of Energy, Borj-Cedria, BP95 Hammams Lif 2050, Tunisia.*

[hmdimohamed@gmail.com](mailto:hmdimohamed@gmail.com)

<sup>\*</sup> *Thermodynamics and Thermal Processes Research Unity, National Engineering School of Monastir, University of Monastir 5019, Tunisia.*

[hmed.taieb@gmail.com](mailto:hmed.taieb@gmail.com)

**Abstract**— In Tunisia, domestic production of organic waste is estimated at 30 million tons per year of which over 1.5 million tons of household waste. This enormous potential can be used efficiently to product electric power. In this context, we investigate numerically the combustion of biogas derived from anaerobic digestion of waste (CH<sub>4</sub>, CO<sub>2</sub>, and N<sub>2</sub>) in a burner of a combustion chamber of an industrial gas turbine. Fluent 6.3-based numerical simulation of methane combustion is validated. Henceforth, we predict the changes in the maximum temperature and emissions in biogas combustion and compare it to natural gas combustion. Results showed that when going from methane to biogas, the flame shape changes considerably and the combustion products increased carbon dioxide concentrations and generated low NO emissions.

**Keywords**— Combustion, anaerobic digestion, flame shape, emissions.

## I. INTRODUCTION

As other countries around the world, Tunisia is aware of the importance of renewable energy and it applies several forms (wind, solar ...etc). Thus, many projects have been launched aimed at cleanliness and improvement of the living environment, as well as the control of pollution from waste disposal. After a first organization of the sector under the organic Law of Municipalities, waste management has evolved through three important steps: From the beginning of the 1990, the establishment of the national waste management program PRONAGDES. The second step is the promulgation of the framework law on waste management in 1996 and the recent creation of a national waste management agency in August 2005, and finally, the elaboration of PRONGIDD referred to the "National Program for the Integrated and Sustainable Management of Waste". In Tunisia, there is about 11.4 million number of inhabitants, 165000 Km<sup>2</sup>, 24 governorates, 264 municipalities and only 35% are rural areas [1-2]. Several studies have been carried out on the waste generated. Annual production are as follows: Household waste: 2.2 million tons per year (0.5 kg/person/day), specific

industrial waste: 150000 tons per year, Phospho-gypsum: 5 million tons per year, 18000 tons per year of waste duty of care and 55000 tons per year of packaging waste [3]. This is due to the simultaneous evolution of three factors: The important economic growth that Tunisia has recorded over the past decades, the strong urbanization and consequently increased pressure on ecosystems and overexploitation of natural resources, and especially the development of standard of living. As depicted by Fig. 1, this development is accompanied by a tremendous growth in electric power consumption which reaches 15 billion kWh on 2014 which meaning 12.75 kwh per capita [4].

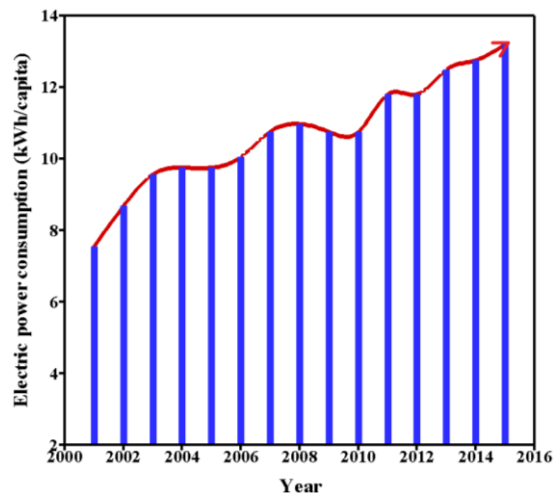


Fig.1 Electric power consumption in Tunisia [2].

Despite the limited funding resources, the national strategy in Tunisia for hazardous waste management can be summarized on the establishment of the list of that wastes according to their specification and origin, the storage and transport of dangerous wastes according to their characteristics, creation of a hazardous waste treatment center for the entire Tunisian territory, the establishment of three regional transfer centers. Also the export of some hazardous

waste abroad by referring to international conventions since their treatment in Tunisia does not present economic profitability. The other strategy aims to recover biogas from landfills. Ministry of Environment and Sustainable Development has initiated studies at the national level to evaluate the deposit of different types of organic waste in order to optimize their recovery methods. This is done by approving of two major Clean Development Mechanism (CDM) projects in the waste management sector (methane flaring in landfills). The project for the recovery and flaring of biogas in the dump of Djebel Chakir which produces 3.2 Metric tons of carbon dioxide equivalent (MtCO<sub>2</sub>) of CH<sub>4</sub>. Biogas recovery and flaring project in 9 controlled discharges (3.7 MtCO<sub>2</sub>), 2 projects that are implemented under the Carbon Fund Prototype managed by the World Bank (Fig. 2).

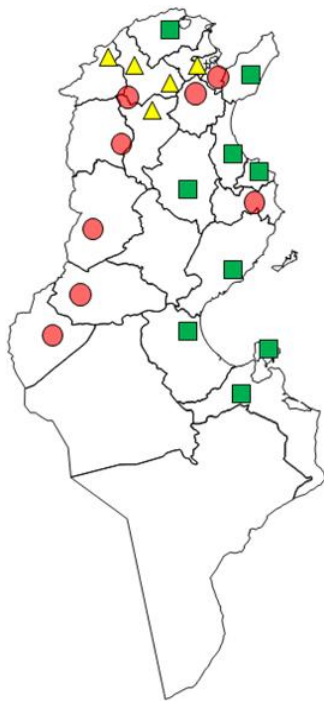


Fig.2 Control and supervision of landfills in Tunisia: ▲ 5 Controlled landfills in the 11th Plan, ■ 9 Controlled discharges and 40 TCs are carried out in the 10th Plan of which 4 are in operation, ● 9 Controlled Discharges and 50 CT are programmed during the 9th Plan [3].

The action program of the National Agency for Energy Conservation (ANME) provides for the development of biogas production at the family level and above from industrial organic waste to a level of contribution to energy production of about 100 Kilo tone of oil equivalent (KTOE) in 2010 [5]. On the other hand, by looking through the production of biogas, the first experiment of introducing biogas in Tunisia was conducted at Sejnène since 1982 as a part of a collaborative project with the German Organisation for Technical Cooperation (GTZ). Another biogas production unit was inaugurated June 10, 2010 in the wholesale market area of Bir El Kasàa. This unit provides an annual energy saving of 108 TOE, an estimated 1.2 m<sup>3</sup> methanization, with extracted organic fertilizer which is intended to organic

farming with a total project cost of 2 million Tunisian dinars (TD) and a capacity production of 2.4 Gigawatt hours (GWh) per year. The electrical energy produced by the unit cover 29% of energy needs of the Tunisian wholesale Market Company (SOTUMAG).

Based on the studies of the master plan for sludge treatment and the evolution of the cost of energy, National Sanitation Office (ONAS) is oriented to broaden the use of biomass to reach other small size STEPs by the creation of centers for the collection, treatment and recovery of sludge and the small sewage treatment plants.

In this context, the biogas combustion is in the heart on operating of electric power generation to fully exploit biogas resulting from waste fermentation. Thus, considerable attention has recently turned to biogas and syngas (products from gasification process) combustion. Many configurations have been studied to illustrate the effects of several parameters on the flow dynamic, flame stability and thermal transfer. Dixon et al. [6] studied numerically and experimentally the conversion of liquid heptane to syngas in a porous medium reactor consisting of a packed bed of alumina pellets. Their results indicated favorable conditions for fuel reforming between equivalence ratios of 2.5 and 3.5 and that the inlet velocity has a significant effect on the performance of noncatalytic fuel reforming. Habib et al. [7] investigated numerically syngas combustion and emission characteristics and compared it with the case of pure methane combustion in a two-burner 200 MW package boiler. Their results showed a combustion delay in case of pure methane combustion as compared to syngas combustion. Also they found that the case of 33% CO:67% H<sub>2</sub> syngas composition having the shortest flame as compared to that of other syngas compositions. Cuoci et al. [8] analyzed three different turbulent non-premixed syngas flames by using different approaches such as the Eddy dissipation (ED) the Eddy dissipation concept (EDC) and steady laminar flamelets (SLF) model. Their results showed that pollutants marginally affect the main combustion process and consequently it is feasible to post-process the CFD results with large detailed kinetic schemes, capable of accurately predicting the formation of pollutants, such as NO<sub>x</sub>, CO, PAH and soot. Gamiño and Aguillón [9] constructed a 2D dynamic model, taking into consideration the turbulent flux combustion reactions of syngas inside a combustion chamber and its displacement through the cylinder of a diesel engine. Their model predicted the profiles of syngas speed, temperature, chemical composition, pressure, and turbulence intensity for the gases when the working parameters and the supply characteristics are modified such as air-syngas ratio, initial temperature of the mixture, initial pressure, compression ratio, and engine speed. Zhang et al. [10] studied 2D numerical simulation of syngas/air combustion under partially premixed combustion (PPC) engine conditions. They found that NO is produced mainly in the premixed burn region, and later from the diffusion burn region in mixtures close to stoichiometry, whereas unburned CO emission is mainly from the diffusion burn region.

## II. PROBLEM DESCRIPTION AND GOVERNING EQUATIONS

### A. Gas turbine combustor configuration

Industrial gas turbine burner is considered here. The burner is designed to burn fuel (biogas in our case) efficiently, reduce emissions, and minimize the wall temperature of the combustion chamber. The size of the burner is 590 mm in the  $z$  direction, 250 mm in the  $y$  direction, and 230 mm in the  $x$  direction (Fig.3). This burner contains six small inlets, each with the surface of  $0.10 \text{ cm}^2$  (equivalent to entries circular with a radius of  $0.18 \text{ cm}$ ). There are also six side air inlets, each with a radius of  $1.5 \text{ cm}$ . This configuration is used by Ghenai [11] to investigate syngas fuel combustion and recently by Guessab et al.[14] to study the combustion of biogas mixtures in the swirl burner can-type. After testing several different meshes, we chose an unstructured mesh consisting of 106321 tetrahedral elements and 31567 nodes. It is refined in regions of strong gradients and properties near solid walls. This is justified by the independence of the solution of the mesh. The primary air ( $F_I=0$ ) has the incoming velocity of  $10 \text{ m.s}^{-1}$  and a temperature of  $300 \text{ K}$ . The fuel ( $F_I=1$ ) is injected with mass flow rate of  $0.001 \text{ Kg.s}^{-1}$  and a temperature of  $300 \text{ K}$ . The secondary air is injected in the combustion chamber through six side air inlets to control the flame temperature and  $\text{NO}_x$  emissions. The injection velocity is  $6 \text{ m/s}$ , the temperature is  $300 \text{ K}$ . The can combustor outlet is maintained at constant relative pressure ( $p=0 \text{ Pa}$ ). For radiation, the P-1 radiation model is used. It must be noted that the P-1 radiation model is the simplest case of the P-N model [12]. The convergence criteria were set to  $10^{-6}$  for all conservation equations.

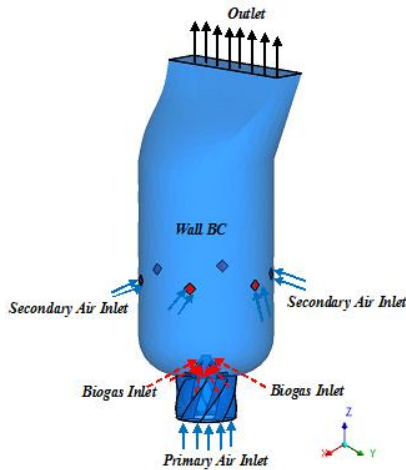


Fig.3 Schematic view of the gas turbine burner.

The main characteristics of the biogas fuel are the lower heating value and the volume of methane produced by the substrate during its anaerobic degradation. Gas turbines are designed primarily to run on natural gas (composed mainly of methane), and providing biogas presents a challenge that must be studied. For this, we must understand the physical and chemical processes of combustion of biogas. The

information, regarding the shape of the flame, the maximum of temperature reached during the combustion and the mass fraction of pollutants  $\text{NO}$  and  $\text{CO}_2$  for a range of biogas compositions is needed for the proper functioning of gas turbine combustors.

### B. Governing Equations

The standard  $k-\varepsilon$  turbulence model [13] is used in this study. The equations for the turbulent kinetic energy  $k$  and the dissipation rate of the turbulent kinetic energy  $\varepsilon$  are solved. For non premixed combustion modeling, the mixture fraction/Probability density function (PDF) model [18] is used. The time-averaged gas-phase equations for steady turbulent flow can be expressed as:

$$\frac{\partial}{\partial x_i} (\rho u_i \Psi) = - \frac{\partial}{\partial x_i} \left( \Gamma_\Psi \frac{\partial \Psi}{\partial x_i} \right) + S \quad (1)$$

Where  $\Gamma_\Psi$  and  $S$  are the effective diffusion coefficient and the source term, respectively.

When  $\Psi = 1$ , we find the continuity equation, while a substitution with  $u$ ,  $v$  and  $w$ , equation (1) represents the momentum equations in the  $x$ ,  $y$  and  $z$  directions, and  $\Psi = k$ , (1) presents the equations of turbulent kinetic energy and dissipation rate of the turbulent kinetic energy which we will present further.

The equation for the conservation of mass can be written as follows:

$$\frac{\partial \overline{\rho u_i}}{\partial x_i} = 0 \quad (2)$$

Conservation of momentum can be described by momentum equation:

$$\frac{\partial \overline{\rho u_i u_j}}{\partial x_j} + \frac{\partial \overline{P}}{\partial x_i} = \frac{\partial}{\partial x_i} (\overline{t_{ij}} + \overline{\tau_{ij}}) \quad (3)$$

$t_{ij}$  is the viscous stress tensor,  $\delta_{ij}$  is the Kronecker symbol  $\delta_{ij} = 1$  if  $i = j$  and  $\delta_{ij} = 0$  if  $i \neq j$ .  $\overline{\tau_{ij}}$  is average Reynolds stress tensor, Boussinesq hypothesis relates the Reynolds stress with the velocity gradients:

$$\overline{\tau_{ij}} = \mu_t \left[ \left( \frac{\partial \overline{u_i}}{\partial x_j} + \frac{\partial \overline{u_j}}{\partial x_i} \right) - \frac{2}{3} \frac{\partial \overline{u_k}}{\partial x_k} \delta_{ij} \right] - \frac{2}{3} \overline{\rho k} \delta_{ij} \quad (4)$$

$\mu_t$  is the turbulent kinetic eddy viscosity and  $k$  is the average turbulent kinetic energy. The constant  $C_\mu$  is given with the commonly used values in the standard  $k - \varepsilon$ ,  $C_\mu = 0.09$ ,  $\overline{\varepsilon}$  is the average dissipation rate of the turbulent kinetic energy. The energy equations can be written in the following form:

$$\frac{\partial (\overline{\rho e + p}) u_j}{\partial x_j} = \frac{\partial \left[ (k + k_t) \frac{\partial \overline{T}}{\partial x_j} \right] - \sum_j h_j J_j + \overline{\varepsilon} e_f u_j}{\partial x_j} + S_h \quad (5)$$

Where  $e$  is the total energy,  $k$  and  $k_t$  are laminar and turbulent thermal conductivity,  $J_j$  is the diffusion flux of species  $j$ , and  $S_h$  is the volumetric heat source.

### III. RESULTS AND DISCUSSIONS

#### A. Combustion of methane

Fig.4 shows the temperature contours at  $x$ - $z$  Plane, and  $y=0$ , the flame height is about 80 mm, The maximum temperature reached in the main flame is 2236 K. The theoretical flame temperature produced by the flame in the initial atmospheric conditions (1 bar and 20 °C) and with a fast combustion reaction (adiabatic flame) of methane is 2233 K [14]. The computation error is then  $Err(\%) = 100 \times \left| \frac{T_{ad} - T_{max}}{T_{ad}} \right| = 0.14$ . This result indicates that no significant differences and the numerical approach compares well with the theoretical adiabatic flame temperature value which indicates how the process of combustion is completed. The chosen turbulent model and other transport equations resolution procedure gives quite satisfactory results. The flame size increases downstream and reaches a maximum radius for  $z=200$  mm. With the increase of the axial distance ( $z=200,300, 445$  mm), the radius and the flame temperature decrease. The lowest gas temperature is reached at the outlet (445 mm) of the burner.

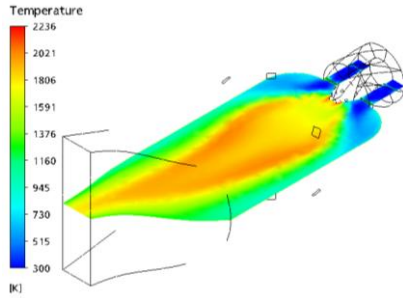


Fig.4 Temperature contour for natural gas combustion.

Fig.5 and Fig.6 show the contours of  $CO_2$  and  $NO$  mass fractions, respectively, produced during the combustion of pure methane. During the combustion and near the secondary air injection zone, the rate of  $CO_2$  reaches its maximum value (0.148) and decreases with the decrease of the temperature of the flame until it reaches the value close to 0.131.

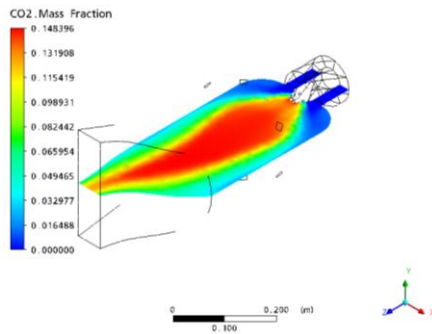


Fig.5  $CO_2$  mass fraction for natural gas combustion.

$CO_2$  mass fraction reaches its maximum value near the secondary air injection zone as the  $O_2$  supply increases in this area, which promotes the combustion process, and is then the  $CO_2$  production.

The fraction of  $NO$  varies according to the  $z$  direction along the axis of the combustor from 0 to  $0.18 \times 10^{-4}$ . It should be noted that the production of  $NO$  which is related to the oxidization of  $N_2$  is favored by the increase in the adiabatic flame temperature: The higher the temperature reached by the reaction, the more pollutant the combustion system is in terms of  $NO_x$ .

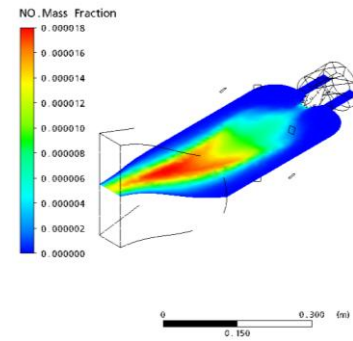


Fig.6  $NO$  mass fraction for natural gas combustion.

#### B. Combustion of biogas

In this section, we aim to study the combustion of biogas derived from anaerobic digestion in the same combustor and compare results with those found using natural gas. The composition of biogas depends on the origin of the products stored and processing conditions. Overall, the biogas containing methane as a main component, carbon dioxide, carbon monoxide, hydrogen sulfide and water. According to their origin, they may also contain varying amounts of nitrogen, oxygen, aromatics, halogenated organic compounds (chlorine and fluorine) and heavy metals (past three chemical families being present in the state of traces). Whatever be their origin, biogas contain flammable and/or toxic gases. Table 2 shows the composition for the three biogas fuel selected for this CFD analysis. Biogas (1) which has the highest fraction of  $CH_4$  comes from industrial effluents. Biogas (2) and biogas (3) come from household waste.

TABLE I  
FLAMMABILITY LIMITS FOR THREE DIFFERENT COMPOSITIONS [16].

$CH_4$ - $CO_2$	Lower Flammability Limit (% v/v $CH_4$ )	Upper Flammability Limit (% v/v $CH_4$ )
60-40	5.1	12.4
55-45	5.1	11.9
50-50	5.3	11.4

Fig.7 shows a contours of temperature ( $x$ - $z$  plane at  $y=0$ ) for methane and the three chosen biogases with different



compositions. The maximum temperature of the tested gases shows a lower value compared with that for the case of methane. This is due to the lower heating value *HV* of biogas compared with pure methane. The maximum temperature reached after combustion of the biogas (a) (68 % CH<sub>4</sub>) is 2219 K. The maximum temperature for the biogas (2) (60% CH<sub>4</sub>) is 2182 K, that is to say 54 K below that of methane. On, biogas (3) maximum temperature is about 2155 K. The biogas (3) is 81 K less than the adiabatic flame temperature for the case of methane. This is due to the decrease in the methane fraction (45%) in the biogas (1). It can be observed that the composition of biogas has an influence on the flame temperature. More biogas contains methane, the more its temperature is high. CH<sub>4</sub> mass fraction decrement in biogas provide a decrease of the flame temperature. The composition of biogas has not only an effect on the maximum temperature within the burner, but also on the shape and the size of the flame. The biogas combustion flame shows a short one compared to that obtained with methane.

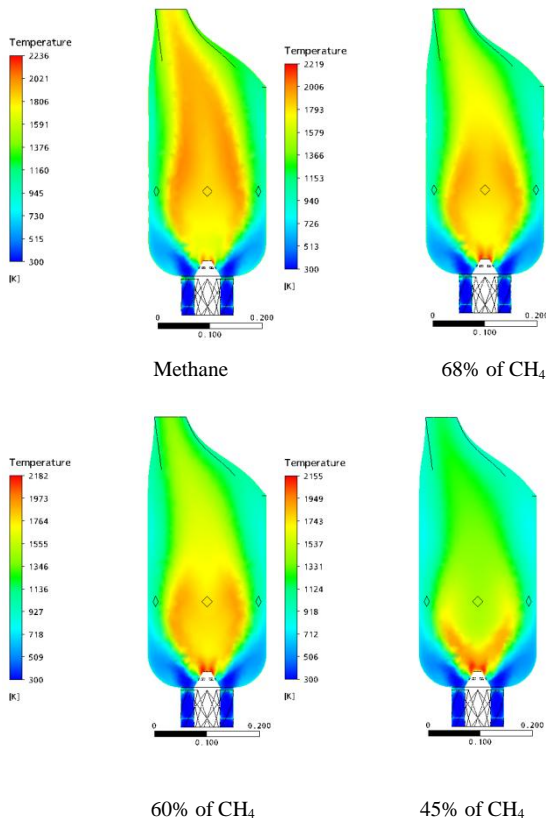


Fig.7 Temperature contour for natural gas 100%, 68%, 60% and 45% of CH<sub>4</sub>.

Table 2 shows the CO<sub>2</sub> and NO mass fraction generated for biogas fuel compared to methane fuel. The presence of inert gases such as N<sub>2</sub> with important quantities in the biogas affects directly the conditions of combustion and emissions. Biogas (1) has the highest mass fraction of carbon dioxide CO<sub>2</sub>. The mass fraction of NO generated from combustion of

biogas (1) and biogas (3) is, respectively,  $7.659 \cdot 10^{-7}$  and  $3.207 \cdot 10^{-7}$ .

TABLE II  
CO<sub>2</sub> AND NO MASS FRACTION GENERATED BY COMBUSTION OF BIOGAS FUEL.

Constituent	Methane	Biogas (1)	Biogas (2)	Biogas (3)
CH <sub>4</sub> (%)	100	68.0	60.0	45.0
CO <sub>2</sub> (%)	0.0	26.0	33.0	32.0
H <sub>2</sub> O (%)	0.0	5.0	6.0	4.0
N <sub>2</sub> (%)	0.0	1.0	1.0	17.0

#### IV. CONCLUSION

In this work, combustion of biogas derived from anaerobic digestion is studied and results are compared with combustion of natural gas. The numerical investigation is done for pure methane (100% CH<sub>4</sub>) and three biogases with different CH<sub>4</sub> and CO<sub>2</sub> mass fractions namely (68% CH<sub>4</sub>+26% CO<sub>2</sub>), (60% CH<sub>4</sub>+33% CO<sub>2</sub>) and (45% CH<sub>4</sub>+32% CO<sub>2</sub>). It has been shown that the increase in the methane mass fraction affects considerably the maximum temperature in the gas turbine combustor, the shape and size of the flame. The combustion of pure methane produces less CO<sub>2</sub> and NO. It can sometimes raise the level of risk, in the absence of appropriate provisions. On the other hand, the highest maximum temperature reached during biogas combustion revealed that biogas can be used in industrial plants as an alternative to natural gas.

#### REFERENCES

- [1] World Bank Data. <http://www.banquemonddiale.org>.
- [2] Central Intelligence Agency (2017). <https://www.cia.gov>.
- [3] National Agency for Waste Management.
- [4] Tunisian national agency for the Control of energy.
- [5] Tunisian Company of Electricity and Gas (STEG).
- [6] M.J. Dixon, I. Schoegl, C.B. Hull and J.L. Ellzey, "Experimental and numerical conversion of liquid heptane to syngas through combustion in porous media", *Combustion and Flame*, vol. 154, pp. 217-231, 2008.
- [7] M.A. Habib, E. M.A. Mokheimer, S. Y. Sanusi and M. A. Nemitallah, "Numerical investigations of combustion and emissions of syngas as compared to methane in a 200 MW package boiler", *Energy Conversion and Management* vol. 83, pp. 296-305, 2014.
- [8] A. Cuoci, A. Frassoldati, G. Buzzi Ferraris, T. Faravelli and E. Ranzi, "The ignition, combustion and flame structure of carbon monoxide/hydrogen mixtures. Note 2: Fluid dynamics and kinetic aspects of syngas combustion", *International Journal of Hydrogen Energy*, vol. 32, pp. 3486-3500, 2007.

- [9] B. Gamiño and J. Aguilón, "Numerical simulation of syngas combustion with a multi-spark ignition system in a diesel engine adapted to work at the Otto cycle", *Fuel*, vol. 89, pp. 581-591, 2010.
- [10] F. Zhang, R. Yu and X.S. Bai, "Detailed numerical simulation of syngas combustion under partially premixed combustion engine conditions", *International journal of hydrogen energy*, vol. 37, pp. 17285-17293, 2012.
- [11] Chaouki Ghenai, "Combustion of Syngas Fuel in Gas Turbine Can Combustor", *Advances in Mechanical Engineering*, pp. 1-13, 2010.
- [12] H. I. Kassem, K.M. Saqr, M.M. Sies and M. Abdul Wahid, "Integrating a simplified P-N radiation model with EdmFoam1.5: Model assessment and validation", *International Communications in Heat and Mass Transfer*, vol. 39, pp. 697-704, 2012.
- [13] B. E. Launder and D. B. Spalding, "Lectures in Mathematical Models of Turbulence", Academic Press, London, England, 1972.
- [14] W. M. Haynes, *CRC Handbook of Chemistry and Physics*, 96th Edition, 2015.